Nat Med. Author manuscript; available in PMC 2016 July 28.

Published in final edited form as:

Nat Med. 2013 December ; 19(12): 1649–1654. doi:10.1038/nm.3372.

Single phosphorylation sites in Acc1 and Acc2 regulate lipid homeostasis and the insulin–sensitizing effects of metformin

Morgan D. Fullerton[1,2,†], **Sandra Galic**[4,†], **Katarina Marcinko**[1,2], **Sarah Sikkema**[1,2], **Thomas Pulinilkunnil**[5], **Zhi–Ping Chen**[4], **Hayley M. O'Neill**[1,2,4], **Rebecca J. Ford**[1,2], **Rengasamy Palanivel**[1,2], **Matthew O'Brien**[4], **D. Grahame Hardie**[6], **S. Lance Macaulay**[7], **Jonathan D. Schertzer**[1,2,3], **Jason R. B. Dyck**[5], **Bryce J. van Denderen**[4], **Bruce E. Kemp**[4], and **Gregory R. Steinberg**[1,2,4,*]

[1]Division of Endocrinology and Metabolism, Department of Medicine, McMaster University, 1280 Main St. W., Hamilton, Ontario, Canada L8N 3Z5

[2]Department of Biochemistry and Biomedical Sciences, McMaster University, 1280 Main St. W., Hamilton, Ontario, Canada L8N 3Z5

[3]Department of Pediatrics, McMaster University, 1280 Main St. W., Hamilton, Ontario, Canada L8N 3Z5

[4]St. Vincent's Institute of Medical Research and Department of Medicine, University of Melbourne, 41 Victoria Parade, Fitzroy, Vic 3065, Australia

[5]Cardiovascular Research Centre, Mazankowski Alberta Heart Institute, Department of Pediatrics, Faculty of Medicine and Dentistry, University of Alberta, T6G 2S2 Edmonton, Alberta, Canada

[6]Division of Cell Signaling & Immunology, College of Life Sciences, University of Dundee, Dundee, DD1 5EH, Scotland, UK

[7]CSIRO Preventative Health Flagship, Materials Science and Engineering, Parkville, Vic 3052, Australia

Abstract

The obesity epidemic has led to an increased incidence of non–alcoholic fatty liver disease (NAFLD) and type 2 diabetes. AMP–activated protein kinase (Ampk) regulates energy homeostasis and is activated by cellular stress, hormones and the widely prescribed anti–type 2

*Correspondence to: Gregory R. Steinberg, Division of Endocrinology and Metabolism, Department of Medicine, HSC 4N63. McMaster University, 1280 Main St. West, Hamilton, Ontario, L8N 3Z5, Canada. Tel: 905.521.2100 ext. 21691, Fax: 905.777.7856, gsteinberg@mcmaster.ca.

†These authors made comparable contributions.

Author Contributions

MDF, SG, BEK and GRS designed the study. MDF, SG, KM, SS, RJF and RP performed *in vivo* experiments. MDF, SG and JDS performed primary hepatocyte experiments. SG, ZC and MO performed Acc activity assays. HMO performed fatty acid oxidation in isolated skeletal muscle. TP and JRD measured tissue malonyl–CoA content. DGH contributed Acc antibodies for activity assays and helpful comments regarding the manuscript. BVD, SLM, BEK and GRS were involved in generating the knock–in mice. MDF and GRS wrote the manuscript.

diabetic drug metformin[1,2]. Ampk phosphorylates murine acetyl–CoA carboxylase[3,4] (Acc) 1 at Ser79 and Acc2 at Ser212, inhibiting the conversion of acetyl–CoA to malonyl–CoA, a precursor in fatty acid synthesis[5] as well as an allosteric inhibitor of fatty acid transport into mitochondria for oxidation[6]. To test the physiological impact of these phosphorylation events we generated mice with alanine knock–in mutations in both Acc1 (Ser79) and Acc2 (Ser212) (Acc double knock–in, AccDKI). These mice have elevated lipogenesis and lower fatty acid oxidation compared to wild–type (WT) mice, which contribute to the progression of insulin resistance, glucose intolerance and NAFLD, but not obesity. Remarkably, AccDKI mice made obese by high–fat feeding, are refractory to the lipid–lowering and insulin–sensitizing effects of metformin. These findings establish that inhibitory phosphorylation of Acc by Ampk is essential for the control of lipid metabolism, and in the setting of obesity, for metformin–induced improvements in insulin action.

Complete genetic disruption of Acc1[7] or Acc2[8–11] has yielded conflicting results as to the role of these enzymes in controlling fatty acid metabolism. The Ampk–mediated phosphorylation of Acc1 at Ser79 (equivalent to Acc2 Ser212) inhibits catalytic activity in cell–free systems[12]. To test the significance of Ampk signaling to Acc *in vivo* we generated Acc1–Ser79Ala and Acc2–Ser212Ala knock–in mice, and inter–crossed these strains to generate AccDKI mice (Supplementary Fig. 1a,b). We examined Ampk–mediated phosphorylation of liver Acc1 Ser79 and Acc2 Ser212 by mass spectrometry and confirmed the absence of phosphorylation at these sites in the AccDKI, but not WT mice (Fig. 1a, Supplementary Fig. 1c). We observed no change in baseline Ampk Thr172 phosphorylation in livers from all three lines and no change in the expression of either Acc isoform (Fig. 1a). The activities of Acc1 and Acc2 were elevated in AccDKI mice (Fig. 1b and c), compared to WT controls; consistent with Ampk phosphorylation negatively regulating Acc1 and Acc2 enzyme activity *in vivo*. Furthermore, lambda phosphatase treatment of liver Acc1 increased enzyme activity in liver from WT, but not AccDKI mice (Supplementary Fig. 2a). Both WT and AccDKI enzymes remained sensitive to citrate activation. Liver malonyl–CoA content is dependent on Acc activity for synthesis and malonyl–CoA decarboxylase (MCD) for degradation. AccDKI mice had elevated liver malonyl–CoA in the fed–state (Fig. 1d), with no compensatory up–regulation of MCD transcript level (Supplementary Fig. 2b) compared to WT control mice. Hepatocytes from AccDKI mice had higher *de novo* lipogenesis (Fig. 1e) and lower fatty acid oxidation (Fig. 1f) compared to WT controls. Consistent with this, AccDKI mice also had higher hepatic *de novo* lipogenesis *in vivo* (Supplementary Fig. 2c) than WT mice. In contrast, single mutations in Acc1 or Acc2 had minimal changes in these parameters, indicating redundancy between Acc isoforms (Supplementary Fig. 2d–f), which is consistent with a previous siRNA knock–down study[10].

Skeletal muscle is the major tissue contributing to the basal metabolic rate, and Acc2 and malonyl–CoA have been shown to be important in regulating skeletal muscle fatty acid oxidation in some[8,13], but not all studies[11,14]. We found that relative to WT controls, malonyl–CoA was higher in skeletal muscle of AccDKI mice (Supplementary Fig. 2g), while fatty acid oxidation was slightly lower (Supplementary Fig. 2h). These data indicate that liver and skeletal muscle malonyl–CoA content, as well as fatty acid metabolism, are sensitive to the regulatory phosphorylation of Acc at Ser79/Ser212.

We examined the phenotype of AccDKI mice fed a standard chow diet. Growth curves (data not shown) and adiposity were similar (Fig. 1g), but liver (Fig. 1h) and skeletal muscle (Supplementary Fig. 2i) diacylglycerol (DAG) and triacylglycerol (TAG) levels were elevated in AccDKI, compared to WT mice. There were no differences in ceramide content in either tissue (data not shown). Elevated hepatic lipid content in AccDKI mice was associated with clinical signs of NAFLD, including an increased level of fibrosis (Fig. 1i) and a slightly elevated serum ALT/AST ratio (Supplementary Fig. 2j), compared to WT controls. Pathological accumulation of DAG has been shown to activate atypical isoforms of protein kinase C (Pkc)[15], where specifically, Pkc–ε and Pkc–δ in liver[16] and Pkc–θ in skeletal muscle[17] have been shown to interfere with canonical insulin signaling. Consistent with this, AccDKI mice had greater membrane associated (Fig. 1j) and phosphorylated Pkc–ε (Supplementary Fig. 3a) in liver and Pkc–θ in skeletal muscle (Supplementary Fig. 3b), compared to control animals, while Pkc–δ was unchanged (data not shown). These results demonstrate that Acc Ser79/Ser212 phosphorylation plays an essential role in preventing ectopic lipid accumulation independent of body mass or adiposity.

The storage of excess lipid in insulin–sensitive organs such as liver and skeletal muscle is strongly associated with insulin resistance[15,18]. We found that AccDKI mice were hyperglycemic (Fig. 2a), hyperinsulinemic (Fig. 2b), and also glucose (Fig. 2c) and insulin intolerant (Fig. 2d), compared to WT controls. Hyperinsulinemic–euglycemic clamp-experiments (Supplementary Fig. 3c) revealed that AccDKI mice had a lower glucose infusion rate (GINF) (Fig. 2e), a lower rate of glucose disposal (GDR) (Fig. 2e), accompanied by elevated hepatic glucose production (HGP) (Fig. 2f) and a lower suppression of HGP by insulin (Fig. 2g), compared to WT controls. Further, livers from AccDKI mice had reduced Akt (Ser473) and FoxO1 (Ser253) phosphorylation (Fig. 2h,i) and higher gluconeogenic gene expression at the completion of the clamp (Fig. 2j), compared to WT controls. c–Jun N–terminal kinase (Jnk), which also inhibits canonical insulin signaling[19], was unchanged in livers from chow-fed AccDKI mice (Supplementary Fig. 3c). We observed a trend towards lower uptake of 2–deoxyglucose (2–DG) into skeletal muscle of AccDKI mice during the clamp (Supplementary Fig. 3d), and a marked reduction in muscle Akt (Ser473) and FoxO1 (Ser253) phosphorylation (Supplementary Fig. 3f,g), measured at the completion of the clamp. Furthermore, insulin resistance in AccDKI mice was independent of changes in liver or adipose tissue macrophage accumulation, inflammatory cytokine gene expression or protein content (Supplementary Fig. 4a–c), or differences in circulating free fatty acids (Supplementary Fig. 4d). These results indicate that Accphosphorylation is required to maintain insulin sensitivity in lean healthy mice.

Over 120 million people are prescribed metformin for the management of type 2 diabetes[20]. Since metformin indirectly activates Ampk, it was initially thought that Ampk mediated metformin's therapeutic actions[21]. However, acute inhibition of gluconeogenesis by metformin is Ampk–independent[22] and involves inhibition of glucagon signaling through protein kinase A (Pka)[23]. Nevertheless, the ability of metformin to lower blood glucose in obese type 2 diabetics involves chronic enhancement in insulin sensitivity[24–27] (see reference[28], a summary of 19 clinical trials), as well as inhibiting glucagon stimulated gluconeogenesis[23]. We found that acute metformin treatment activated hepatic Ampk in both genotypes, but this was only associated with increased Acc phosphorylation (Fig. 3a) and

reduced malonyl–CoA levels (Fig. 3b) in WT mice. Metformin reduced *de novo* lipogenesis in hepatocytes from WT mice, and this suppressive effect was equivalent to that caused by Ampk β1–specific activation using A–769662[29] (Fig. 3c). Importantly, the metformin–induced inhibition of hepatic lipogenesis seen upon Ampk activation was entirely mediated by Ampk phosphorylation of Acc, as metformin and A–769662 were ineffective at suppressing lipogenesis in AccDKI or *Ampk–β1*$^{-/-}$ hepatocytes (Fig. 3c). However, unlike A–769662, metformin did not increase fatty acid oxidation in either genotype (Supplementary Fig. 4e). These data demonstrate that the effects of metformin on lipogenesis are specific for Ampk, and indicate that while Ampk may inhibit multiple targets in this pathway, including sterol regulatory element binding protein 1c[30] and expression of fatty acid synthase[31], the primary regulation of lipogenesis is dependent on the phosphorylation of both Acc1 and Acc2. In contrast, lipogenesis was inhibited by metformin in hepatocytes from both WT and Acc1KI mice (Supplementary Fig. 4f) and *in vivo*, a lipid–lowering effect was demonstrated in HFD–fed WT and Acc1KI animals treated with metformin (Supplementary Fig. 4g). Notably, mice with complete deletions of Ampk isoforms in skeletal muscle[32] or liver[22] have normal lipid levels and insulin sensitivity, suggesting that in these models, there may be alterations in compensatory pathways that are important for controlling fatty acid metabolism.

In humans, therapeutic doses of metformin (0.5–3 g/day)[26], result in plasma concentrations ranging from 10–25 μM[33,34]. In rodents, the administration of 50 mg/kg of metformin has been shown to elicit plasma concentrations of 29 μM[35]. We therefore treated obese WT and AccDKI mice with a daily dose of metformin (50 mg/kg) for 6 weeks. In contrast to chow–fed mice, HFD–fed AccDKI mice showed no differences in any metabolic parameters compared to HFD–fed WT animals (Fig. 3 and Supplementary Figs. 5–7). This indicates that diet–induced obesity overwhelms the effect of signaling by endogenous Ampk to Acc, unless an external Ampk stimulus is provided.

Metformin has been shown to have positive effects on fatty liver in some, but not all clinical trials[24]. However, rodent studies with metformin have demonstrated a clear lipid–lowering effect[21,29], which suggests the need for more robust analyses or the development of more reliable biomarkers in human studies[24,36]. Notably, *in vivo* lipogenesis was similar between HFD–fed WT and AccDKI mice (Fig. 3d), and an acute dose of metformin (50 mg/kg) suppressed *in vivo* lipogenesis by ~ 35% in WT livers, yet was completely ineffective in AccDKI mice (Fig. 3d). We next assessed the metabolic effects of chronic metformin treatment and showed that independent of change in weight or adiposity (Supplementary Fig. 5c) hepatic lipid content was reduced in WT mice, an effect completely absent in AccDKI mice (Fig. 3e–g). Reductions in hepatic DAG, were accompanied by decreased membrane–associated (Fig. 3h) and Ser729 phosphorylated Pkc–ε (Supplementary Fig. 5d) and lower Jnk activation (Supplementary Fig. 5e) in metformin–treated WT, but not AccDKI mice.

In addition to reducing hepatic lipid content, chronic metformin treatment of obese WT, but not obese AccDKI mice, was associated with lowered fasting blood glucose (Fig. 4a), a trend toward lowered serum insulin levels (Supplementary Fig. 5f), and improved glucose tolerance (Supplementary Fig. 5g) and insulin sensitivity (Fig. 4b). Metformin–induced

suppression of cAMP and glucagon–dependent hepatic glucose output is Ampk–independent[22,23], and in hepatocytes from WT, AccDKI and *Ampk–β1*$^{-/-}$ mice, metformin was effective at suppressing cAMP–stimulated glucose production (Supplementary Fig. 5h). Metformin was also able to acutely lower circulating glucose levels in both chow and obese HFD–fed, WT and AccDKI mice, as shown by metformin–tolerance tests (200 mg/kg[37]) (Supplementary Fig. 5i). However, at the dose that was utilized for our chronic treatments (50 mg/kg), glucose levels were unaltered (Supplementary Fig. 5j), strongly suggesting that metabolic differences following chronic metformin treatment between AccDKI and WT mice were primarily the result of differential regulation of insulin sensitivity rather than acute effects on glucose lowering.

In hyperinsulinemic–euglycemic clamp experiments, chronic metformin treatment improved GDR (Supplementary Fig. 6a) and skeletal muscle 2–DG uptake in both WT and AccDKI mice (Supplementary Fig. 6b,c). This is consistent with an Ampk/Pkc–dependent pathway controlling metformin–induced skeletal muscle glucose uptake[38]. In contrast, chronic metformin treatment increased GINF (Supplementary Fig. 6d–g), decreased HGP (Fig. 4c) and increased suppression of HGP by insulin (Fig. 4d) in WT, but not AccDKI mice. Enhanced Akt (Ser473) and FoxO1 (Ser253) phosphorylation (Supplementary Fig. 7a,b) and reduced gluconeogenic gene expression (Supplementary Fig. 7c) at the completion of the clamp in WT, but not in AccDKI mice, provides further evidence of metformin–induced improvements in hepatic insulin sensitivity. Notably the ability of metformin to improve insulin sensitivity was demonstrated to be liver cell–autonomous in a cellular model of palmitate–induced insulin resistance. Hepatocytes made insulin–resistant by chronic treatment (18 h) with the saturated fatty acid palmitate, were co–treated with metformin, which improved insulin stimulated phosphorylation of Akt Ser473 and FoxO1 Ser253 (Fig. 4e), insulin–induced suppression of gluconeogenic gene expression (Fig. 4f), as well as insulin–induced suppression of hepatic glucose production (Fig. 4g) in hepatocytes from WT, but not AccDKI mice. Importantly, the beneficial metabolic effects of specific Ampk activation via A–769662, were completely abrogated in AccDKI hepatocytes and *in vivo* (Supplementary Fig. 8a–d) and corroborates the fundamental importance of Ampk/Accsignaling for hepatic lipid metabolism and insulin sensitivity.

Metformin remains the primary therapeutic option for the treatment of type 2 diabetes, although the precise mechanisms by which it confers its beneficial effects are incompletely understood. Glucagon–driven hepatic gluconeogenesis maintains glycemia during states of fasting and this is poorly regulated in type 2 diabetic patients. Recently, it was demonstrated that metformin counters this program by inhibiting glucagon–stimulated cAMP production, thereby reducing PKA activity and glucagon–stimulated glucose output from the liver[23]. We confirmed this mechanism also operates in both WT and AccDKI mice in response to high concentrations of metformin (Supplementary Fig. 8e). An important distinction between previous work[23] and our study was their focus on the fasting/glucagon–specific mechanisms of metformin, which occur in the absence of insulin stimulation. The ability of insulin to suppress hepatic gluconeogenesis, as well as to promote the efficient uptake of glucose in the periphery is fundamental and dramatically decreased in insulin resistance and type 2 diabetes. The insulin–sensitizing effects of metformin have been well documented[24,27,28], but mechanistic insight has been lacking. Our data provide clear evidence that in the setting

of obesity and insulin resistance, chronic metformin treatment (at a physiological dose) reduces hepatic lipogenesis and lipid accumulation via activation of Ampk and consequent inhibition of both Acc1 and Acc2. This lipid–lowering effect then alleviates obesity–induced insulin resistance. Notwithstanding metformin inhibition of glucagon–dependent gluconeogenesis, we provide evidence for a parallel mechanism, whereby chronic metformin treatment increases insulin sensitivity via alterations in hepatic lipid homeostasis (Fig. 4h).

Since the initial discovery that Ampk directly phosphorylates Acc1, more than 30 substrates have been identified, thus making it difficult to determine the metabolic pathways by which this multi–substrate kinase regulates insulin sensitivity and lipid metabolism. Moreover, the site–specific phosphorylation of Acc1 and Acc2, has been used as a surrogate marker for Ampk signaling in hundreds of studies over the past decade. Through genetic targeting of Acc1 Ser79 and Acc2 S212, representing the first knock–in mice generated for any Ampk substrates, we show that phosphorylation and inhibition of Acc is critical not only for maintaining lipid metabolism and insulin sensitivity, but also underpins the insulin–sensitizing effects of metformin.

Online Methods

Animals

Both Acc1–S79A KI and Acc2–S212A KI mice were generated by OzGene Pty Ltd, (Perth Australia). The targeting strategy is summarized in Supplementary Fig S1. The generation of *Ampk–β1*$^{-/-}$ and *Ampk–β2*$^{-/-}$ mice has previously been described[39,40]. All mice used in the study were bred on a C57Bl/6 background and were bred from heterozygous intercrosses. Male mice were used for all studies and housed in SPF micro–isolators and maintained on a 12 h light/dark cycle with lights on at 0700. Mice were maintained on either a chow (17% kcal from fat; Diet 8640, Harlan Teklad, Madison, WI) or HFD (45% kcal from fat, D12451, Research Diets; New Brunswick, NJ) starting at 6 weeks of age for 12 weeks. For HFD–metformin experiments, mice received 6 weeks of daily intraperitoneal injections of metformin (50 mg/kg) starting after 6 weeks of the HFD. Fasting and fed blood samples were collected for serum analyses via submandibular bleeding. The McMaster University (Hamilton, Canada) Animal Ethics Research Board and St. Vincent's Hospital (Melbourne, Australia) Animal Ethics Committee approved all experimental protocols.

Enzymatic activity assays

Acc activity in liver or gastrocnemius was measured by $^{14}CO_2$ fixation into acid–stable products. Acc1 and Acc2 protein was precipitated from 2 mg of tissue homogenates using antibodies specific for either Acc1 or Acc2. Antibodies against Acc1 and Acc2 were generated by immunizing sheep with synthetic peptides coupled to keyhole limpet hemocyanin (CDEPSPLAKTLELNQ (rat Acc1 (1–15 Cys^{1}) and CEDKKQAPIKRQLMT (rat Acc2 (145–159 Cys^{145})) and purifying antibodies from the resulting sera by affinity chromatography on immobilized peptides. Immunoprecipitates were incubated for 1.5 h at room temperature with reaction buffer containing 125 μM acetyl–CoA, 12.5 mM $NaHCO_3$ and 16.7 μCi/ml [^{14}C]–$NaHCO_3$ with the indicated concentrations of citrate. The reactions were terminated by addition of HCl and dried overnight at 37 °C. Water was added to the

dried sample and radioactivity measured by liquid scintillation counting. Purified Acc1 protein from WT and Acc1 KI livers were subjected to λ phosphatase (400 U in a 60 μl reaction) treatment for 25 min at 30 °C. After a wash removal of the phosphatase, a small aliquot was used for determination of Acc1 Ser79 phosphorylation via Western blot. The majority of the protein that remained was used to assess Acc activity, as described above.

Mass spectrometry analyses

Acc isoforms from WT and AccDKI livers were affinity purified by Straptavidin Sepharose. Proteins were eluted from beads, reduced and alkylated with iodacetamide, then precipitated with methanol:chloroform (1:1, v/v). The denatured proteins were digested overnight with trypsin in solution at 37 °C. Peptides were separated on a PepMap RSLC C18 column using a Dionex 3000 Series NCS–3500RS nano liquid chromatography system. Mass spectrometry was performed on a 5600 Triple TOF MS (Ab–Sciex).

Malonyl–CoA Assay

Quantification of short chain CoA species was performed as reported previously with modification[41]. Briefly, frozen muscle and liver samples (~15–20 mg) were homogenized for 20 sec in 300 μl of 6% (v/v) Perchloric acid. After homogenization, the samples were left on ice for 10 min and then centrifuged at 12,000 *g* for 5 min. 100 μl of the resulting supernatant was used for UPLC analysis by a Water's Acquity system. Each sample was run at a flow rate of 0.4 ml/min through an Ascentis express column C18, 10 cm × 2.1 mm and 2.7 μm particle size from Supelco maintained at a temperature of 40 °C. The analyte detection occurred at an absorbance of 260 nm. The mobile phase consisted of a mixture of buffer A (0.25 M NaH_2PO_4 and water) and buffer B (0.25 M NaH_2PO_4 and acetonitrile). The gradient elution profile consisted of the following initial conditions (2% B; 2–4 min 25% B; 4–6 min 40% B; 6–8 min 100% B; 10–12 min) maintained for 15 min. All gradients were linear and peaks were acquired, integrated and analyzed using the Waters Empower Software.

Histological analyses

Tissues were fixed in formalin for at least 48 h, embedded in paraffin and H&E stained. After staining, each sample was imaged in triplicate. For determination of hepatic fibrosis, trichrome staining was used to visualize collagen. This was then quantified using the color segmentation function of Image J software (NIH).

Western blotting, inflammation and real time quantitative PCR

Tissues were dissected rapidly, snap frozen in liquid nitrogen and stored at −80 °C until subsequent analyses. Blotting for total and phosphorylated Akt, Jnk, Ampk and Acc (antibodies all from Cell Signaling) were performed as previously described[42]. Phosphorylated FoxO1 Ser 253, was normalized to Gapdh (Cell Signaling). For Pkc–ε phosphorylation, an antibody directed against Ser729 was used (Abcam). For membrane–associated Pkc activation, tissues were homogenized in 300 μl of buffer I (20 mM Tris·HCl, pH 7.4, 1 mM EDTA, 0.25 mM EGTA, 250 mM sucrose and protease inhibitor mixture) and centrifuged at 100,000 × g for 1 h (4 °C). The supernatants containing the cytosolic fraction

were removed to new tubes. Pellets were then resuspended in 300 μl of buffer II (250 mM Tris·HCl, pH 7.4, 1 mM EDTA, 0.25 mM EGTA, 2% Triton X 100, protease inhibitor mixture) and centrifuged at 100,000 × g for 1 h (4 °C) to obtain the plasma membrane fraction. Gapdh and caveolin–1 were used as markers of the cytosolic and membrane preparation purity, respectively. Pkc activation is expressed as a ratio of membrane (normalized to caveolin–1) to cytosolic (normalized to Gapdh) localization, which was assessed from the same membrane to eliminate exposure bias. Hepatic tissues were prepared as previously described[43] and pro–inflammatory cytokines were determined using commercially available kits. Total RNA isolation, cDNA synthesis and quantitative real time PCR were performed as described previously[42].

Metabolic studies

For glucose, insulin and metformin tolerance tests, mice were injected with D–glucose (2 g/kg and 1 g/kg for chow and HFD, respectively), human insulin (0.6 U/kg and 1 U/kg for chow and HFD, respectively) or 50 and 200 mg/kg metformin[37] via IP injection and blood glucose monitored at the indicated times by a small cut in the tail vein. Whole body adiposity was assessed by computed tomography and respiratory exchange ratio was determined using Columbus Laboratory Animal Monitoring System, as previously described[42]. Hyperinsulinemic–euglycemic clamps were performed as previously described[42]. Briefly, 5 days post–cannulation, only mice that lost < 8% of their weight were clamped. Mice, fasted 6 h were infused with a basal infusate containing D–[3–^{3}H]–glucose (7.5 μCi/h, 0.12 ml/h) for 1 h to determine basal glucose disposal. An insulin infusate (10 mU/kg/min insulin in 0.9% saline) containing D–[3–^{3}H]–glucose (7.5 μCi/h, 0.12 ml/h) was then initiated and blood glucose monitored and titrated with 50% dextrose infused at a variable rate to achieve and maintain euglycemia. For rates of glucose uptake, [^{14}C] 2–deoxyglucose (10 μCi) was infused during the clamped state and tissues excised after 30 min. The rates of glucose disposal in the basal and clamped states as well as hepatic glucose output were calculated using Steele's equation for steady state conditions[44]. Insulin was measured by ELISA kit, ALT and AST were determined using commercially available kits and TAG levels were determined by glycerol assay following saponification of the TAG fraction separated using thin layer chromatography. Total levels of tissue DAG and ceramides were quantified using DAG kinase assay as previously described[45]. *De novo* lipogenesis was determined *in vivo* by the incorporation of [^{3}H]–acetate into hepatic lipids after metformin (50 mg/kg) or A769662 (30 mg/kg), where saline and 5% DMSO in PBS served as vehicles, respectively. Skeletal muscle fatty acid oxidation was assessed in isolated EDL muscles as previously described[40]. For metformin–stimulated glucose uptake, isolated EDL muscles were incubated with either: vehicle (60 min), metformin (1 mM for 60 min), submaximal insulin (2.0 μM for 30 min) or metformin (1 mM for 60 min) plus insulin (2.0 μM for 30 min). 2–DG uptake was then measured over 20 min in the presence of insulin (2 μM) or metformin (1 mM). To measure hepatic cAMP, WT and AccDKI mice in the fed condition were injected with vehicle, 200 or 400 mg/kg metformin. After 1 h, mice received a vehicle or glucagon injection (2 mg/kg). Livers were collected after 5 min and rapidly freeze–clamped[23]. Hepatic cAMP measurements were performed using an EIA from Cayman Chemicals, and was used as per the manufactures instructions.

Cell culture experiments

Primary hepatocytes were isolated by collagenase perfusion[42]. [^{3}H]–acetate lipogenesis and [^{14}C]–palmitate oxidation was performed as described previously[39]. Briefly, for lipogenesis [^{3}H]–acetate (5 μCi/ml) was in the presence of 0.5 mM sodium acetate for 4 h. Media was then removed and cells washed with PBS prior to lipid extraction for determination of incorporation into lipid fractions. For fatty acid oxidation, [^{14}C]–palmitate (2 μCi/ml) was in the presence of 0.5 mM palmitate (conjugated to 2% BSA) for 4 h. Media was removed and acidified with equal volume of 1 M acetic acid in an air–tight vial. [^{14}C]–CO_2 was trapped in 400 μl of 1 M benzethonium hydroxide and radioactivity determined. Cellular lipids were extracted after a PBS wash and radioactivity of the acid soluble intermediates was determined. Total oxidation was then calculated as a function of both [^{14}C]–CO_2 produced and incomplete oxidation products. For insulin signaling experiments in hepatocytes, cells were incubated in the presence or absence of 0.5 mM palmitate (conjugated to 2% BSA) and 0.5 mM metformin for 18 h (with 0.1% FBS). Cells were then stimulated with 10 nM insulin, where gluconeogenic gene expression was assessed after 6 h of insulin treatment and insulin signaling was assessed after 5 min of insulin stimulation. Hepatic glucose production was determined as previously described[22]. Briefly, cells were cultured as above, in the presence of 100 nM dexamethasone. Cells were washed once with PBS and incubated in glucose–free DMEM (100 nM dexamethasone, 10 mM lactate, 1 mM pyruvate) ± Bt_2–cAMP (100 μM) ± indicated doses of metformin or A769662. For chronic treatments, palmitate–, metformin– and A769662–supplemented media was removed after 18 h, cells were washed and glucose–free DMEM was added to measure glucose output in the presence or absence of insulin (10 nM). Glucose in the media after 4 h was assessed by glucose oxidase kit.

Statistical analysis

All results shown are mean ± standard error of the mean (SEM). Results were analyzed using a two–tailed Student's *t* test or two–way ANOVA where appropriate, using GraphPad Prism software. A Bonferonni *post hoc* test was used to test for significant differences revealed by the ANOVA. Significance was accepted at $P \leq 0.05$.

Supplementary Material

Refer to Web version on PubMed Central for supplementary material.

Acknowledgments

We thank C. Saab from the McMaster Centre for Translational Imaging for completing the CT analysis and S. Stypa and E. Day for technical assistance. These studies were supported by grants and fellowships from the Australian Research Council and CSIRO (BEK), Australian National Health and Medical Research Council (BEK, BVD and GRS), the Canadian Diabetes Association (GRS, JRD and JDS) and the Canadian Institutes of Health Research (CIHR) (GRS and JRD). Supported in part by the Victorian Government's OIS Program (BEK) and Canadian Foundation for Innovation (GRS). MDF is a CIHR Banting Postdoctoral Fellow, JDS is a CDA Scholar and GRS is a Canada Research Chair in Metabolism and Obesity.

References

1. Kahn BB, Alquier T, Carling D, Hardie DG. AMP-activated protein kinase: ancient energy gauge provides clues to modern understanding of metabolism. Cell metabolism. 2005; 1:15–25. [PubMed: 16054041]
2. Long YC, Zierath JR. AMP-activated protein kinase signaling in metabolic regulation. J Clin Invest. 2006; 116:1776–1783. [PubMed: 16823475]
3. Carlson CA, Kim KH. Regulation of hepatic acetyl coenzyme A carboxylase by phosphorylation and dephosphorylation. The Journal of biological chemistry. 1973; 248:378–380. [PubMed: 4692841]
4. Carling D, Zammit VA, Hardie DG. A common bicyclic protein kinase cascade inactivates the regulatory enzymes of fatty acid and cholesterol biosynthesis. FEBS letters. 1987; 223:217–222. [PubMed: 2889619]
5. Wakil SJ, Stoops JK, Joshi VC. Fatty acid synthesis and its regulation. Annual review of biochemistry. 1983; 52:537–579.
6. McGarry JD, Leatherman GF, Foster DW. Carnitine palmitoyltransferase I. The site of inhibition of hepatic fatty acid oxidation by malonyl-CoA. The Journal of biological chemistry. 1978; 253:4128–4136. [PubMed: 659409]
7. Abu-Elheiga L, et al. Mutant mice lacking acetyl-CoA carboxylase 1 are embryonically lethal. Proceedings of the National Academy of Sciences of the United States of America. 2005; 102:12011–12016. [PubMed: 16103361]
8. Abu-Elheiga L, Matzuk MM, Abo-Hashema KA, Wakil SJ. Continuous fatty acid oxidation and reduced fat storage in mice lacking acetyl-CoA carboxylase 2. Science. 2001; 291:2613–2616. [PubMed: 11283375]
9. Harada N, et al. Hepatic de novo lipogenesis is present in liver-specific ACC1-deficient mice. Molecular and cellular biology. 2007; 27:1881–1888. [PubMed: 17210641]
10. Savage DB, et al. Reversal of diet-induced hepatic steatosis and hepatic insulin resistance by antisense oligonucleotide inhibitors of acetyl-CoA carboxylases 1 and 2. J Clin Invest. 2006; 116:817–824. [PubMed: 16485039]
11. Hoehn KL, et al. Acute or chronic upregulation of mitochondrial fatty acid oxidation has no net effect on whole-body energy expenditure or adiposity. Cell metabolism. 2010; 11:70–76. [PubMed: 20074529]
12. Munday MR, Campbell DG, Carling D, Hardie DG. Identification by amino acid sequencing of three major regulatory phosphorylation sites on rat acetyl-CoA carboxylase. European journal of biochemistry/FEBS. 1988; 175:331–338.
13. Choi CS, et al. Continuous fat oxidation in acetyl-CoA carboxylase 2 knockout mice increases total energy expenditure, reduces fat mass, and improves insulin sensitivity. Proceedings of the National Academy of Sciences of the United States of America. 2007; 104:16480–16485. [PubMed: 17923673]
14. Olson DP, Pulinilkunnil T, Cline GW, Shulman GI, Lowell BB. Gene knockout of Acc2 has little effect on body weight, fat mass, or food intake. Proceedings of the National Academy of Sciences of the United States of America. 2010; 107:7598–7603. [PubMed: 20368432]
15. Erion DM, Shulman GI. Diacylglycerol-mediated insulin resistance. Nature medicine. 2010; 16:400–402.
16. Samuel VT, et al. Inhibition of protein kinase Cepsilon prevents hepatic insulin resistance in nonalcoholic fatty liver disease. J Clin Invest. 2007; 117:739–745. [PubMed: 17318260]
17. Yu C, et al. Mechanism by which fatty acids inhibit insulin activation of insulin receptor substrate-1 (IRS-1)-associated phosphatidylinositol 3-kinase activity in muscle. The Journal of biological chemistry. 2002; 277:50230–50236. [PubMed: 12006582]
18. Chibalin AV, et al. Downregulation of diacylglycerol kinase delta contributes to hyperglycemia-induced insulin resistance. Cell. 2008; 132:375–386. [PubMed: 18267070]
19. Hirosumi J, et al. A central role for JNK in obesity and insulin resistance. Nature. 2002; 420:333–336. [PubMed: 12447443]

20. Viollet B, et al. Cellular and molecular mechanisms of metformin: an overview. Clin Sci (Lond). 2012; 122:253–270. [PubMed: 22117616]
21. Zhou G, et al. Role of AMP-activated protein kinase in mechanism of metformin action. J Clin Invest. 2001; 108:1167–1174. [PubMed: 11602624]
22. Foretz M, et al. Metformin inhibits hepatic gluconeogenesis in mice independently of the LKB1/AMPK pathway via a decrease in hepatic energy state. J Clin Invest. 2010; 120:2355–2369. [PubMed: 20577053]
23. Miller RA, et al. Biguanides suppress hepatic glucagon signalling by decreasing production of cyclic AMP. Nature. 2013
24. Musso G, Cassader M, Rosina F, Gambino R. Impact of current treatments on liver disease, glucose metabolism and cardiovascular risk in non-alcoholic fatty liver disease (NAFLD): a systematic review and meta-analysis of randomised trials. Diabetologia. 2012; 55:885–904. [PubMed: 22278337]
25. Bailey CJ, Mynett KJ. Insulin requirement for the antihyperglycaemic effect of metformin. British journal of pharmacology. 1994; 111:793–796. [PubMed: 7912625]
26. Bailey CJ, Turner RC. Metformin. The New England journal of medicine. 1996; 334:574–579. [PubMed: 8569826]
27. Gomez-Samano MA, et al. Metformin improves the hepatic insulin resistance index independently of anthropometric changes. Endocrine practice: official journal of the American College of Endocrinology and the American Association of Clinical Endocrinologists. 2011:1–24.
28. Natali A, Ferrannini E. Effects of metformin and thiazolidinediones on suppression of hepatic glucose production and stimulation of glucose uptake in type 2 diabetes: a systematic review. Diabetologia. 2006; 49:434–441. [PubMed: 16477438]
29. Cool B, et al. Identification and characterization of a small molecule AMPK activator that treats key components of type 2 diabetes and the metabolic syndrome. Cell metabolism. 2006; 3:403–416. [PubMed: 16753576]
30. Li Y, et al. AMPK phosphorylates and inhibits SREBP activity to attenuate hepatic steatosis and atherosclerosis in diet-induced insulin-resistant mice. Cell metabolism. 2011; 13:376–388. [PubMed: 21459323]
31. Foretz M, Carling D, Guichard C, Ferre P, Foufelle F. AMP-activated protein kinase inhibits the glucose-activated expression of fatty acid synthase gene in rat hepatocytes. The Journal of biological chemistry. 1998; 273:14767–14771. [PubMed: 9614076]
32. O'Neill HM, et al. AMP-activated protein kinase (AMPK) beta1beta2 muscle null mice reveal an essential role for AMPK in maintaining mitochondrial content and glucose uptake during exercise. Proceedings of the National Academy of Sciences of the United States of America. 2011; 108:16092–16097. [PubMed: 21896769]
33. Lalau JD, Lemaire-Hurtel AS, Lacroix C. Establishment of a database of metformin plasma concentrations and erythrocyte levels in normal and emergency situations. Clinical drug investigation. 2011; 31:435–438. [PubMed: 21401215]
34. Owen MR, Doran E, Halestrap AP. Evidence that metformin exerts its anti-diabetic effects through inhibition of complex 1 of the mitochondrial respiratory chain. The Biochemical journal. 2000; 348(Pt 3):607–614. [PubMed: 10839993]
35. Wilcock C, Bailey CJ. Accumulation of metformin by tissues of the normal and diabetic mouse. Xenobiotica; the fate of foreign compounds in biological systems. 1994; 24:49–57. [PubMed: 8165821]
36. Clark JM, Brancati FL, Diehl AM. Nonalcoholic fatty liver disease. Gastroenterology. 2002; 122:1649–1657. [PubMed: 12016429]
37. He L, et al. Metformin and insulin suppress hepatic gluconeogenesis through phosphorylation of CREB binding protein. Cell. 2009; 137:635–646. [PubMed: 19450513]
38. Turban S, et al. Defining the contribution of AMP-activated protein kinase (AMPK) and protein kinase C (PKC) in regulation of glucose uptake by metformin in skeletal muscle cells. The Journal of biological chemistry. 2012; 287:20088–20099. [PubMed: 22511782]
39. Dzamko N, et al. AMPK beta1 deletion reduces appetite, preventing obesity and hepatic insulin resistance. The Journal of biological chemistry. 2010; 285:115–122. [PubMed: 19892703]

40. Steinberg GR, et al. Whole body deletion of AMP-activated protein kinase {beta}2 reduces muscle AMPK activity and exercise capacity. The Journal of biological chemistry. 2010; 285:37198–37209. [PubMed: 20855892]
41. Ussher JR, et al. Stimulation of glucose oxidation protects against acute myocardial infarction and reperfusion injury. Cardiovascular research. 2012; 94:359–369. [PubMed: 22436846]
42. Galic S, et al. Hematopoietic AMPK beta1 reduces mouse adipose tissue macrophage inflammation and insulin resistance in obesity. J Clin Invest. 2011; 121:4903–4915. [PubMed: 22080866]
43. Schertzer JD, et al. NOD1 activators link innate immunity to insulin resistance. Diabetes. 2011; 60:2206–2215. [PubMed: 21715553]
44. Steele R. Influences of glucose loading and of injected insulin on hepatic glucose output. Annals of the New York Academy of Sciences. 1959; 82:420–430. [PubMed: 13833973]
45. Preiss J, et al. Quantitative measurement of sn-1,2-diacylglycerols present in platelets, hepatocytes, and ras- and sis-transformed normal rat kidney cells. The Journal of biological chemistry. 1986; 261:8597–8600. [PubMed: 3013856]

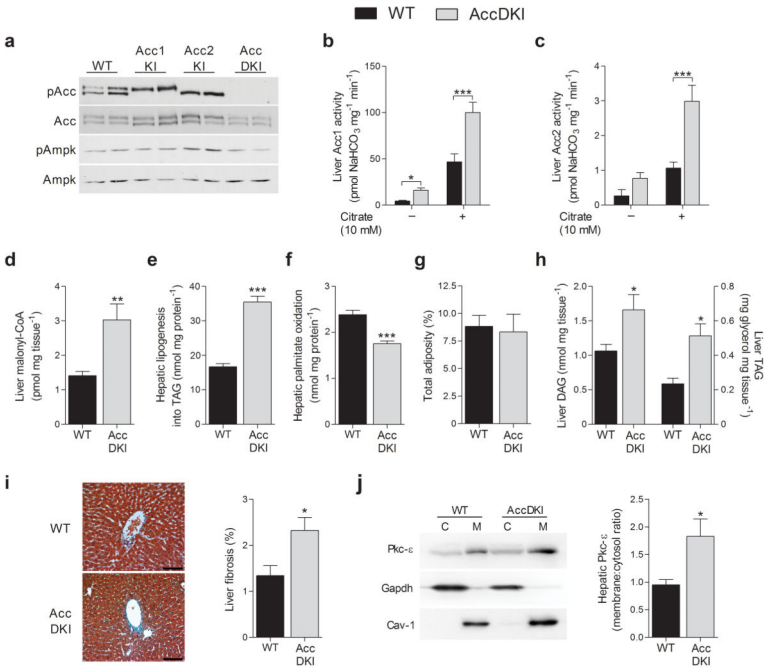

Fig. 1. Acc1 Ser79 and Acc2 Ser212 are essential for inhibiting enzyme activity and regulating liver fatty acid metabolism

(**a**) Representative Western blot of Ampk–αThr172, zcc1 Ser79 (bottom band) and Acc2 Ser212 (top band) phosphorylation in liver of WT, Acc1KI and Acc2KI and AccDKI mice. (**b**) Acc1 and (**c**) Acc2 activity with and without citrate (10 mM) in WT and AccDKI liver (n = 5 WT and 6 DKI). (**d**) Liver malonyl–CoA in the fed–state (n = 8). (**e**) The incorporation of [^{3}H]–acetate into TAG as a measure of *de novo* lipogenesis and (**f**) [^{14}C]–palmitate oxidation in primary hepatocytes (n = 3, from at least 3 separate experiments). (**g**) Total adiposity in chow-fed WT and AccDKI (n = 10 WT and 14 DKI). (**h**) Liver DAG and TAG (n = 6 WT and 8 DKI). (**i**) Histological representation (scale bar is 100 μm) and quantification of collagen staining in liver sections (n = 6). (**j**) Activation of liver Pkc–ε as demonstrated by membrane–association (n = 7). Data are expressed as means ± SEM, * P < 0.05, ** P < 0.01 and *** P < 0.001 relative to WT, as determined by ANOVA and Bonferonni *post hoc* test or a Student's t test. For Pkc activation, Gapdh and caveolin–1 were used for cytosolic and membrane normalization, respectively, and blots shown are from duplicate gels.

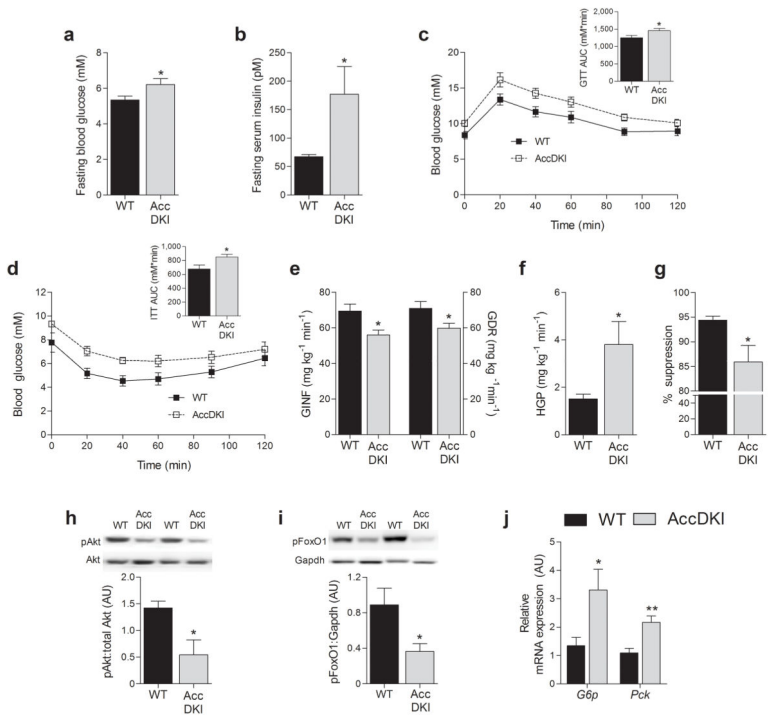

Fig. 2. AccDKI mice fed a control diet are glucose intolerant and have hepatic insulin resistance

(**a**) Fasting blood glucose, (**b**) fasting serum insulin levels, (**c**) glucose tolerance test (2 g/kg) and (**d**) insulin tolerance test (0.6 U/kg) (n = 10 WT and 14 DKI) in WT and AccDKI mice. Hyperinsulinemic–euglycemic clamp results: (**e**) glucose infusion rate (GINF) and glucose disposal rate (GDR), (**f**) hepatic glucose production (HGP), and (**g**) suppression of hepatic glucose production (n = 7 WT and 8 DKI). (**h**) Liver Akt (Ser473) phosphorylation, (**i**) liver FoxO1 (Ser253) phosphorylation and (**j**) gluconeogenic gene expression (*G6p* and *Pck*) in the liver at the completion of the clamp (n = 7 WT and 8 DKI). Data are expressed as means ± SEM, * $P < 0.05$ and ** $P < 0.01$ relative to WT, as determined by Student's t test. Relative gene expression was normalized to *Actb* and duplicate gels were run for quantification of total Akt and Gapdh.

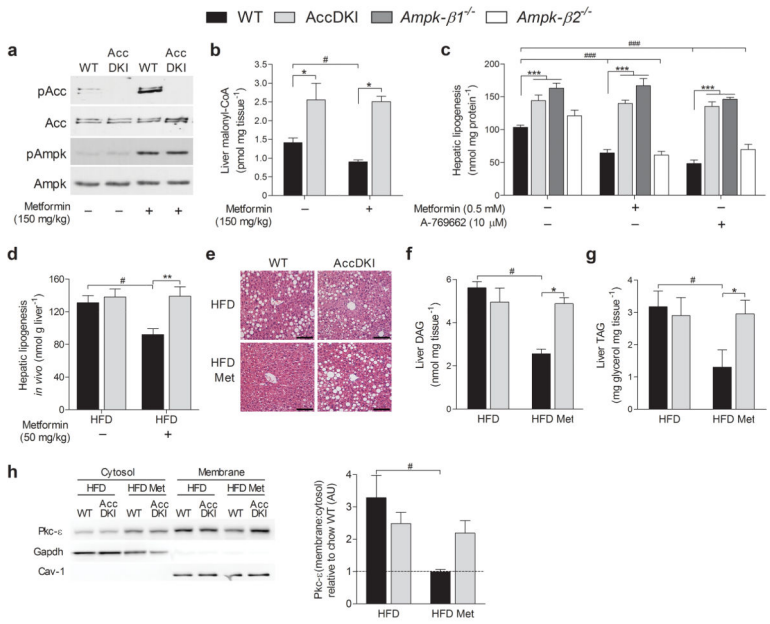

Fig. 3. Metformin improves hepatic lipid metabolism via inhibition of Acc

(**a**) Ampk and Acc phosphorylation and (**b**) liver malonyl–CoA levels from saline– or metformin– (150 mg/kg) injected WT and AccDKI mice in the fed–state (n = 6 WT and 8 DKI). (**c**) Incorporation of [^{3}H]–acetate into the total lipid fraction (*de novo* lipogenesis) in primary hepatocytes (n = 3 from at least 3 separate experiments). (**d**) *In vivo* incorporation of [^{3}H]–acetate into total liver lipid (*de novo* lipogenesis) in HFD–fed WT and AccDKI mice treated with vehicle or metformin (50 mg/kg) (n = 11 for vehicle and n = 6 for metformin). (**e**) Representative staining (H&E) of hepatic sections (scale bar is 100 μm) as well as determination of hepatic (**f**) DAG and (**g**) TAG (n = 7 WT and 8 DKI) from WT and AccDKI mice fed a HFD for 12 weeks, with or without concurrent metformin (50 mg/kg/day) starting after 6 weeks of HFD diet. (**h**) Activation of hepatic Pkc–ε, shown as the ratio of membrane/cytosolic expression and expressed relative to chow WT control (n = 7) (cytosol normalized to Gapdh and membrane normalized to caveolin–1; blots shown are from duplicate gels). Data are expressed as means ± SEM, * $P < 0.05$, ** $P < 0.01$, and *** $P < 0.001$ compared to WT control and $^{\#}$ $P < 0.05$ and $^{\#\#\#}$ $P < 0.01$ are differences between treatment, as calculated by two–way ANOVA and Bonferonni *post hoc* test.

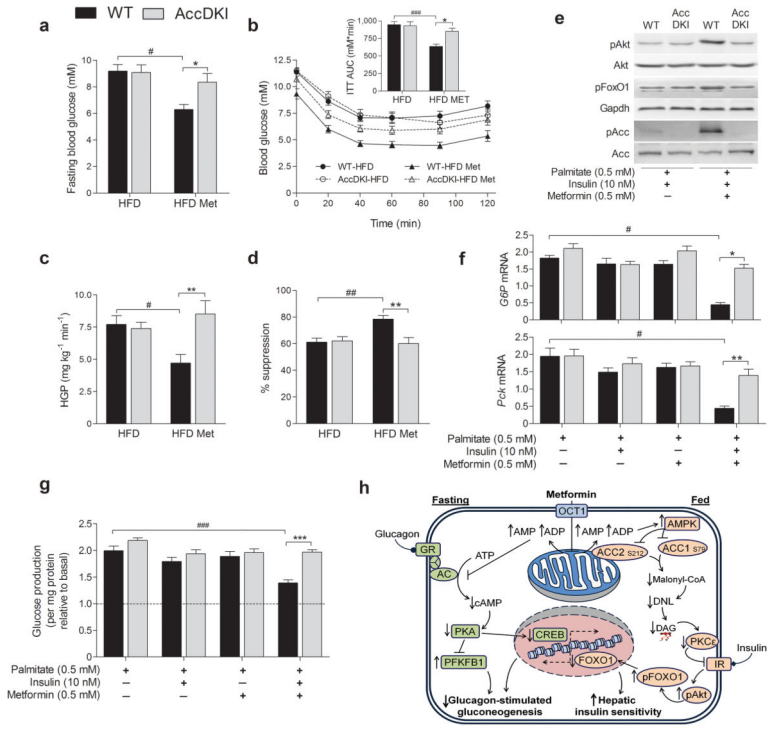

Fig. 4. Obese AccDKI mice are insensitive to metformin–induced improvements in liver insulin sensitivity

WT and AccDKI mice fed a HFD for 6 weeks were given daily metformin (50 mg/kg) for an additional 6 weeks. (**a**) Fasting blood glucose and (**b**) insulin tolerance test (1 U/kg) (n = 10 HFD–fed WT and DKI; n = 12 WT and 16 DKI HFD–metformin). The effect of metformin treatment on (**c**) hepatic glucose production (HGP) and (**d**) suppression of HGP by insulin (n = 7 WT and 9 DKI). (**e**) Akt (Ser473) and FoxO1 (Ser253) phosphorylation, as well as (**f**) *G6p* and *Pck* expression, in isolated hepatocytes treated with chronic palmitate (18 h) and stimulated with insulin, where gene expression is shown relative to the WT condition without palmitate. (**g**) Hepatic glucose production, following chronic (18 h) exposure to palmitate (0.5 mM) in the presence or absence of metformin (0.5 mM), then in response to Bt_2–cAMP (100 μM) and insulin (10 nM) for 4 h, in the absence of acute metformin. (n = 3, from at least 3 separate experiments). Hatched line represents control hepatocytes not stimulated with Bt_2–cAMP for glucose production. (**h**) Schematic representation of metformin's therapeutic effects on hepatic action during differential nutrient and hormonal programs. Data are expressed as means ± SEM, * $P < 0.05$, ** $P < 0.01$ and *** $P < 0.001$ represent differences between genotype and $^{\#}$ $P < 0.05$, $^{\#\#}$ $P < 0.01$ and $^{\#\#\#}$ $P < 0.001$ are differences between treatment, as calculated by two–way ANOVA and Bonferonni *post hoc* test.